

Synthesis and characterization of magnesium doped titania for photocatalytic degradation of methyl red

Samreen Zahra¹, Sania Mazhar², Sarwat Zahra³,
Hira Idrees⁴, Ali Hussnain⁵

¹PCSIR Laboratories Complex, Mineral Processing Research Centre, Ferozpur Road, Lahore, 54600, Lahore, Punjab, Pakistan

²PCSIR Laboratories Complex, Food and Biotechnology Research Centre, Ferozpur Road, Lahore, 54600, Lahore, Punjab, Pakistan

³University of Education, Lahore, Department of Physics, DSNT, College Road Township, Lahore, 54770, Lahore, Punjab, Pakistan

⁴University of Education, Lahore, Department of Chemistry, DSNT, College Road Township, Lahore, 54770, Lahore, Punjab, Pakistan

⁵Minhaj University Lahore, Department of Physics, Township, Lahore, 54770, Lahore, Punjab, Pakistan
e-mail: samreenzahra68@hotmail.com, saniamazhar@gmail.com, sarwat.zahra@ue.edu.pk, hiraidrees09@gmail.com, ah.shah14@gmail.com

ABSTRACT

Magnesium doped titania (MDT) composites with varying magnesium weight percentages (1-5 wt. %) were synthesized through a very simple and economical route of sol-gel method. The reactants used for making alkoxide precursor were titanium tetrachloride whereas magnesium nitrate was used for doping magnesium into titania in a mixture of solvents i.e. ethyl alcohol and water. The optimum conditions maintained for preparing sol were pH 3 and 60 °C temperature with constant stirring for 2 hours. The gel obtained after drying the sol for each sample was calcined at 500 °C for two hours. The powdered composite samples thus prepared were characterized by X-ray diffraction analysis (XRD), differential scanning calorimetry-thermogravimetric analysis (DSC-TGA), infrared spectroscopy (IR), scanning electron microscopy (SEM) and energy dispersive X-ray spectroscopy (EDX). The samples were evaluated for their photocatalytic activity against methyl red dye under UV light irradiation and the dye degradation was examined by UV-Vis spectrophotometer. The results confirmed the excellent photocatalytic activity of synthesized magnesium doped TiO₂ for the degradation of methyl red dye where MDT-3 having 3% magnesium doping exhibited the maximum degradation i.e. 96.8%.

Keywords: Magnesium doped titania, Sol-gel method, photocatalytic activity.

1. INTRODUCTION

Nowadays, there has been a growing interest in the search of nanosize materials beneficial for various mechanical, electrical, magnetic, optical, chemical, biological and pharmaceutical applications. Nanomaterials of different shapes and sizes especially, metal oxides have attracted considerable attention owing to their distinct physicochemical properties. Among these, titanium dioxide (TiO₂) has emerged as one of the most attractive metal oxides which is nontoxic, low-cost and environment friendly in addition to its distinct semiconducting and photocatalytic properties. Hence, it has been successfully used as pigment, catalyst in solar cells, sunscreens, drugs and pharmaceuticals. Titania has also been extensively used as antimicrobial agent for water and air samples owing to its sufficient photocatalytic activity essential for destroying a variety of microorganisms [1-4].

The antimicrobial properties of titania can be enhanced by incorporating small quantities of metals into it for example gold, silver, iron and zinc etc. that are also well-known as antimicrobial agents [5] but an adverse effect owing to the health hazardous nature of metals has minimized their use [6]. Moreover, the use of coinage metals involves high production cost and makes these materials quite expensive. Therefore, new possible environment friendly and cost effective substitutes have to be explored [7]. Organic antimicrobial agents are also known to have various side effects, including their toxicity and instability at elevated tem-

perature and pressure. In contrast to organic compounds used as antimicrobial agents, the inorganic compounds are chemically stable and heat resistant [5].

Metal doped titania has been produced by several routes including sol-gel, chemical vapor deposition, ion-assisted sputtering, chemical mixing, magnetron sputtering and ion implantation [8]. However, the most commonly applied method is sol-gel being simple and capable of producing a variety of structures just by controlling process parameters [9]. Scientists have prepared pure as well as doped titania nanoparticles through aqueous and nonaqueous routes of sol-gel technique. For example, KEDZIORA *et al.* synthesized undoped as well as doped titania nanoparticles via sol-gel method and confirmed their excellent antibacterial activity [10]. GUPTA and co-workers reported sol-gel prepared titania and silver doped titania and compared their structural and optical properties as well as antimicrobial activity against both gram positive and gram negative bacteria [11]. TOBALDI *et al.* also prepared Ag-modified titania nanoparticles by a green aqueous sol-gel method and found them to exhibit good photocatalytic activity and enhanced antibacterial activity against *Escherichia coli* (Gram-negative) and methicillin-resistant *Staphylococcus aureus* (Gram-positive) bacteria [12]. Since, sol-gel synthesis of supported silver nanoparticles leads to a product having highly dispersed active silver over a large surface area therefore, this approach allows it to be used as an efficient antibacterial agent utilizing a lower quantity of silver metal [13]. Titanium dioxide doped with transition metals like Fe and Co has also been prepared by the previous scientists by sol-gel method [1, 14]. STOYANOVA *et al.* developed iron and copper doped titania nanoparticles for their potential use as antibacterial agents [15]. CHEKURI and co-workers synthesized various concentrations of cobalt doped titania nanopowders following a surfactant free approach and found them reasonably photocatalytically active for the degradation of azo dye Acid Red as well as an exceptional antibacterial agent against *Escherichia coli* [16].

Dopants also may include nonmetals like sulphur, nitrogen, carbon etc. for enhanced physical properties of titanium dioxide [17]. ZANE *et al.* determined the efficiency of nitrogen-doped titania nanoparticles as antibacterial agent when exposed to blue light [18]. In another study, scientists evaluated carbon and nitrogen doped titanium dioxide immobilized on glass support for investigating the inactivation of *Escherichia coli* ATCC 25922 bacteria in water [19]. Similarly, WONG *et al.* confirmed that as compared to pure TiO₂ nitrogen-doped TiO₂ exhibit greater bacterial activity against *E. coli* and in killing a variety of pathogens under visible-light illumination. These findings proved that nitrogen-doped TiO₂ has potential for being applied as disinfectant used in the fields of health and environment [20].

Owing to the fact that the modified titania powders absorb more visible light radiations and consequently possess higher antibacterial activity as compared to pure TiO₂ particles, titania doped with nonmetals like carbon, nitrogen, boron and fluorine, together with binders including wear resistant polymers are being used to make microbe-free surface coatings generally employed for fruit and vegetable containers [21]. Similarly, nanotitania modified food packaging films have been developed to produce antimicrobial and photocatalytic food packaging with toxin passivation in order to preserve food safely [22]. Other titania base nanomaterials with enhanced photocatalytic and antibacterial activities have also been developed by the previous scientists for example, doped titania nanorods, silica/titania nanospheres, silver doped titania sol-gel films, Ag doped TiO₂-chitosan (STC) prepared by the inverse emulsion cross-linking reaction, Ag-TiO₂ composite nanofilms on silicon wafer synthesized by sol-gel spin-coating technique, Cu-doped titanium dioxide thin films on glass substrate, sulfur-doped titania thin films prepared by atmospheric pressure chemical vapour deposition, silver-nanostructures coated TiO₂ thin films on pure titania, carbon-doped TiO₂ and nitrogen-doped TiO₂ substrates using thermal reduction method, TiO₂(N)/Ag/TiO₂(N) sandwich films containing silver embedded between two TiO₂(N) layers [23-31].

Present study is therefore aimed at the synthesis of different compositions of magnesium doped titania composite powders by a simple, cheap and environment friendly process i.e. sol-gel method. The prepared samples were characterized by XRD, DSC-TGA, IR, SEM and EDX techniques. The prepared samples were evaluated against methyl red dye for their potential use as photocatalyst for environmental applications.

2. MATERIALS AND METHODS

2.1 Materials

All the reagents used i.e. titanium tetrachloride, magnesium nitrate, isopropyl alcohol and ethyl alcohol used were of analytical grade.

2.2 Sample preparation

Different compositions of magnesium doped titania were synthesized by aqueous route of sol-gel process shown in the flowchart (Figure 1). The sols were prepared by dissolving titanium tetrachloride in isopropyl alcohol taken in stoichiometric ratio, diluting the sol with ethyl alcohol and water taken in 1:2 ratio.

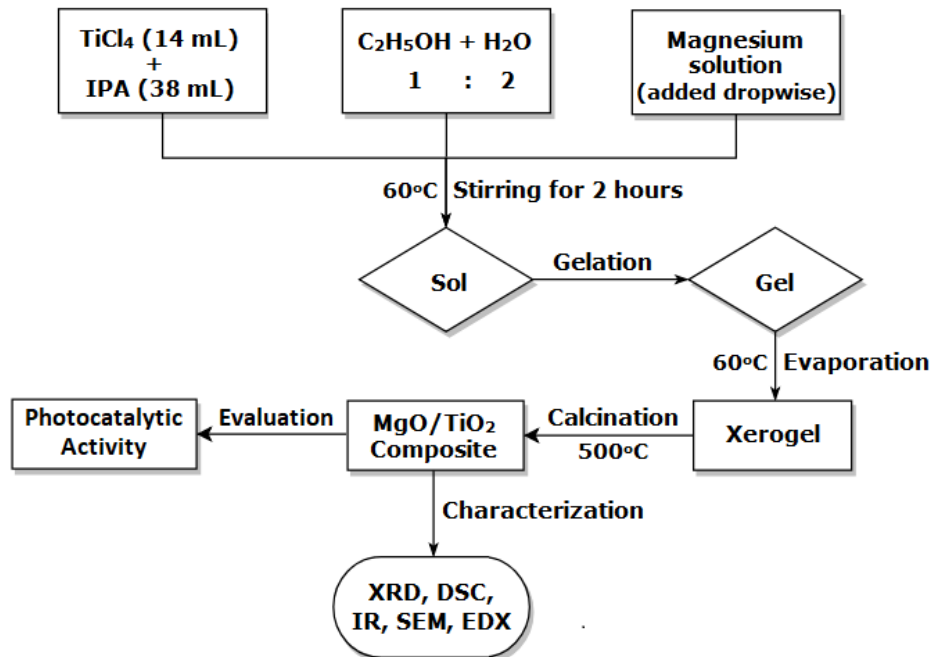


Figure 1: Flow diagram for the synthesis of MDT samples.

A known quantity of magnesium nitrate solution prepared in water was then added dropwise to the mixture at 60°C and pH 3 with constant stirring for two hours. The sols thus obtained were dried at 60°C for 24 hours and after grinding the samples were calcined at 500°C for two hours. Four compositions (MDT-1, MDT-2, MDT-3 and MDT-4) of titania doped with variable quantities of magnesium (1%, 2%, 3% and 5%) were prepared.

2.3 Characterization

The prepared samples were characterized by PANalytical X'Pert PRO X-ray diffractometer using monochromatised $\text{CuK}\alpha 1$ radiation having wavelength of 1.54060\AA . Thermal analysis was carried out using differential thermal analyzer Universal V4.5A, TA instruments USA, under nitrogen atmosphere from room temperature to 1000°C at a rate of 10°C/min. Infrared spectroscopy was performed with Thermo Nicolet IR 200 (USA), the samples were scanned through Zinc Selenide (Zn-Se) ATR. The surface morphology of the samples along with energy dispersive X-ray spectroscopy were performed using scanning electron microscope S-3700N Hitachi Japan.

2.4 Photocatalytic activity

The photocatalytic activity of as prepared MDT samples was evaluated by the degradation of methyl red (MR) dye. The experiments were performed by adding 50 mg of each MDT sample to 100 ml of 100 ppm methyl red aqueous solution. Each mixture was stirred in dark for 30 minutes at room temperature to reach adsorption equilibrium. The mixtures in glass containers were then kept under 366 nm UV-Vis illumination using Desager Sarstedt-Gruppe, MiniUVis photoreactor, 4-5 cm away from the UV lamp inside a black box to prevent leakage. The tests were carried out at room temperature for 60 minutes during the irradiation. After that the samples were centrifuged at 5000 rpm for 20 minutes and were analyzed with the UV-Vis spectrophotometer at 522 nm. The percentage degradation of MR solutions was calculated from the following equation:

$$\text{Degradation (\%)} = [1 - A_t/A_0] \times 100 \quad [1]$$

where, A_t is the absorbance at time t and A_0 is the initial absorbance of MR before degradation [32].

3. RESULTS AND DISCUSSION

3.1 X-ray diffraction analysis

The prepared samples of magnesium doped titania i.e. MDT-1, MDT-2, MD-3 and MDT-4, calcined at 500°C were evaluated by X-ray diffraction technique in order to determine their phase compositions and diffractograms are shown in Figure 2 (a, b, c & d). All the peaks were identified by matching with JCPDS files 78-2485, 87-0920 and 45-0946 that confirmed the crystalline nature of all the four samples.

Figure 2a shows distinct peaks of tetragonal anatase and rutile phases of titania at 2θ values 25.53° and 27.77° respectively. However, the peak for anatase appears to be relatively less intense. Also, the smaller peaks at 36.43° , 48.09° , 54.57° , 55.29° , 62.91° and 69.03° represent the anatase phase. Similarly, the peak of less intensity at 2θ values 41.49° and 44.15° indicate the rutile phase. However, more peaks that can be assigned to the rutile phase of titania that appear at 2θ values 36.07° , 54.31° , 56.62° , 62.75° , 68.99° , and 69.79° cannot be seen distinctly hence it can be said that peaks for both the phases were superimposed by each other and hence resulted in broadening of peaks. All these observations are in accordance with those reported by the former scientists [33, 34].

SHIVARAJU and co-workers also had similar observations and obtained mixed phases of titania while synthesizing Mg-doped TiO_2 polyscales and concluded that it is due to the influence of Mg dopant incorporated into titania crystals. They also observed that the XRD pattern for titania doped with magnesium varies from that of pure TiO_2 and shows broadening of peaks [35]. Figure 2a also illustrates minor peak at 2θ value 37.57° that confirms the presence of cubic structure of magnesium oxide. Other diffraction peaks that appear at 2θ values 42.9° , 62.28° and 74.65° as observed by the previous scientists for pure magnesium oxide [36, 37] cannot be seen distinctly, they might also be overlapped by the peaks for titania.

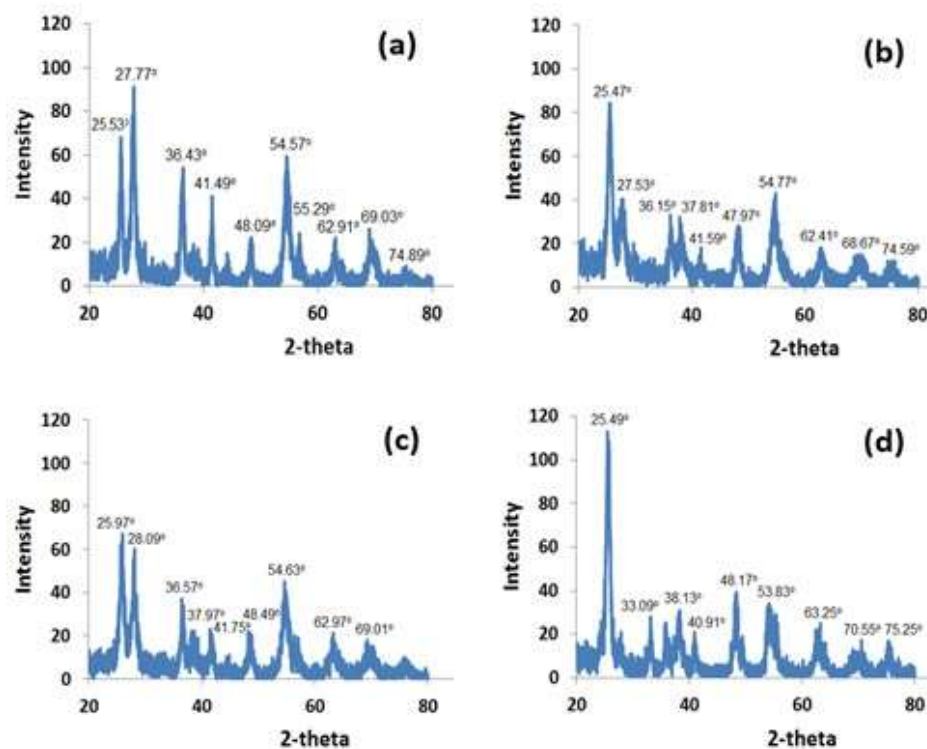


Figure 2: X-ray diffraction patterns (a) MDT-1; (b) MDT-2; (c) MDT-3; (d) MDT-4.

Similar diffraction peaks can be observed in case of all MDT samples but with a slight variation in intensities except MDT-4, the XRD pattern for which reveals one distinct peak for anatase phase of titania at 2θ value 25.49° whereas the peak around 2θ value 27.77° totally disappears indicating the complete transformation of titania into anatase phase. This observation leads to the conclusion that rise in the percentage of MgO inhibits the transformation of anatase to rutile phase and higher calcination temperature may be required for the transformation of titania to the more stable rutile phase. No peak for the intermediate brookite phase of titania is observed in any sample. Hence, MDT-1, MDT-2 and MDT-3 contain mixtures of two

phases of titania i.e. anatase and rutile whereas MDT-4 contains purely anatase phase of titania. As concluded by the previous scientists that photocatalytic activity improves when anatase and rutile phases co-exist owing to the utilization of electron-hole pairs among interconnecting particles of both the phases [38].

3.2 Thermal analysis

Thermal behavior of synthesized MDT samples was studied by DSC-TGA and curves are shown in Figures 3a, 3b, 3c and 3d. The TGA curve (Figure 3a) shows a gradual and continuous weight loss of 30.91% with three main stages of decomposition in case of MDT-1. The first stage below 150 °C comprising of 6.78% weight loss that occurs due to the evaporation of adsorbed water and solvent [38-40]. The major weight loss of 12.77% that is seen between 150 °C and 500 °C is assigned to the removal of moisture and organic residues captured by the mesopores present between the crystallite aggregates.

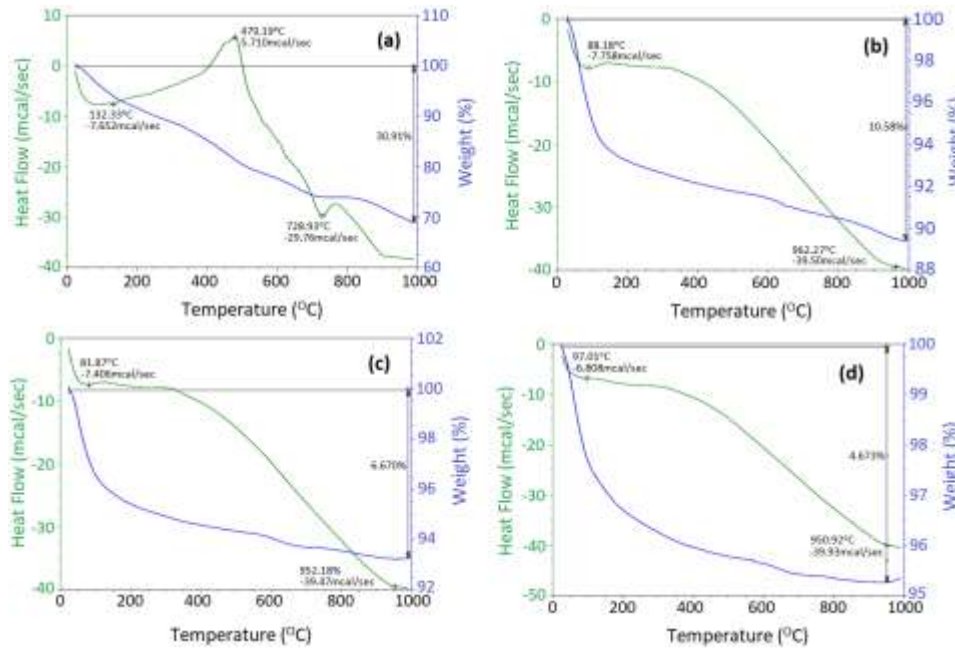


Figure 3: DSC-TGA curves (a) MDT-1; (b) MDT-2; (c) MDT-3; (d) MDT-4.

As observed by the previous researchers that complete decomposition of organic residues occurs above 150 °C and below 500 °C since organic compounds are absorbed chemically by the material synthesized through the sol-gel process and subsequently desorbed at these temperatures [41-44]. This weight loss may also be attributed to the decomposition of residual nitrate group since magnesium nitrate was used as precursor for doping magnesium into titania matrix. The third variation of 11.36% loss in mass from 500°C to 1000°C corresponds to the phase change from anatase to rutile titania [45].

In case of MDT-2 (Figure 3b), a total weight loss of 10.58% is observed; a first step of 6.29% below 150 °C due to moisture loss and the second variation of 4.29% from 150 °C to 1000 °C attributed to the removal of entrapped moisture and organic impurities as well as the phase change in anatase titania. MDT-3 and MDT-4 show almost similar behavior with relatively less variation in weight i.e. 6.67% and 4.67% respectively (Figures 3c & 3d) with major weight loss below 150 °C indicating the removal of physically adsorbed moisture; negligible variation in weight can be observed in both the samples from 150 °C to 1000 °C proving their highly crystalline structure and thermal stability.

DSC curve for MDT-1 in Figure 3a shows a broad endothermic peak below 150 °C that confirms the removal of adsorbed water [40, 46]. The curve exhibits a broad plateau shaped exothermic peak between 150 °C and 500 °C ascribed to the volatilization of chemisorbed water and organic residues [39, 47]. Yodyingyong *et al.* also observed the broad exothermic peak from 100 °C to 500 °C related to the decomposition of volatile organic solvents [48]. Another endothermic peak of relatively high intensity is seen between 500 °C and 1000 °C due to slow phase transformation of anatase to rutile titania [40, 46]. Some previous scientists also found lowering of transition temperature to 708 K and 858 K that takes place due to magnesium doping of titania [49].

The DSC curve for MDT-2 (Figure 3b) illustrates quite different thermal behavior as compared to MDT-1. Though a similar endothermic peak related to the removal of adsorbed water is observed below 150

°C but after that no exothermic peak can be seen between 150 °C and 500 °C, instead the endothermic peak continues from 150 °C to 1000 °C with a gradual but continuous change in heat absorbed by the sample that corresponds to the volatilization of entrapped or chemisorbed water and organic remainders along with the phase transformation of anatase titania. MDT-3 and MDT-4 also show similar behavior as observed in case of MDT-2 (Figure 3c & 3d).

The results show that as the percentage of dopant is increased the total weight loss in each MDT sample decreases till it reaches 4.67% in case of MDT-4 containing 5% magnesium probably due to a denser microstructure and lower surface area. This observation reveals that the thermal stability of doped titania samples increases with the percentage of dopant. Moreover, no significant weight loss at higher temperatures is observed confirming the formation of highly crystalline and stable MDT samples.

3.3 Infrared spectroscopy

IR spectra of synthesized MDT samples i.e. MDT-1, MDT-2, MDT-3 and MDT-4 were recorded in the frequency range of 4000-400 cm^{-1} and are presented in Figures 4 (a, b, c & d) respectively. The spectra show similar absorption bands with slight variation in intensities among all the MDT samples. Several strong bands can be seen in the region 3800-3000 cm^{-1} , this region is related to the stretching vibrations of numerous hydroxyl groups i.e. free O-H groups present on the surface of samples, O-H groups of adsorbed water molecules and also, hydrogen bonded O-H groups. The region from 3800-3600 specifies the stretching vibrations of free O-H groups adsorbed on the surface of titania nanoparticles [43, 50-52].

The absorption bands between 3000-2800 cm^{-1} are attributed to the symmetric and asymmetric stretching vibrations of alkyl groups of organic compounds entrapped in the crystals during their formation [38, 53]. Several less intense absorption bands that appear in the region 2800-2200 cm^{-1} correspond to the presence of strong hydrogen bonding among water molecules. However, the minor absorption bands centered at 1624 cm^{-1} and 1627 cm^{-1} observed among all the MDT samples are associated with the bending vibrational modes of hydroxyl groups of water molecules [34, 54-56]. Other minor bands at 1386 cm^{-1} appear due to the asymmetric stretching vibrations of nitrate group [57].

The broad absorption band featured from 1000 cm^{-1} to 400 cm^{-1} in each MDT sample is assigned to the stretching vibrations of Ti-O and Ti-O-Ti bonds [38, 56]. The absorption band observed between 1100-1000 cm^{-1} in each spectrum corresponds to the vibrational modes of Ti-O-Mg bond that confirms the composite formation [53]. The shift of Ti-O-Mg vibration at an increased frequency as compared to Ti-O-Ti bond can be attributed to the lower mass of magnesium as compared to titanium. Liu et al. concluded for the similar absorption band at 1105 cm^{-1} that it appears due to the bending vibrational mode of Ti-O-Mg instead of O-Mg [59].

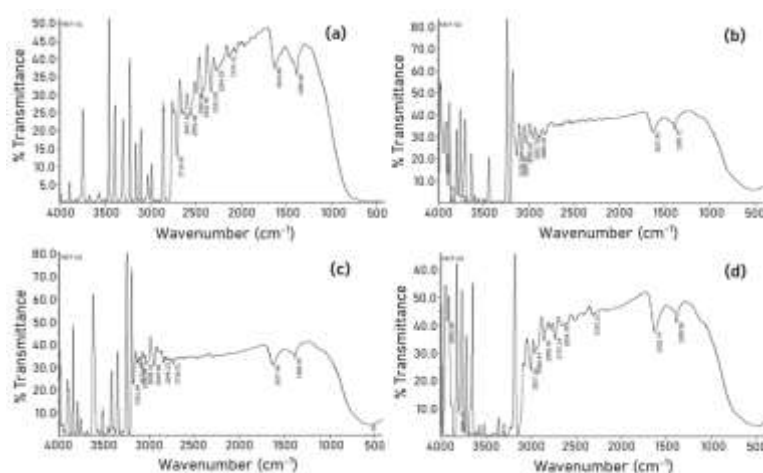


Figure 4: Infrared spectra (a) MDT-1; (b) MDT-2; (c) MDT-3; (d) MDT-4.

Hence, the results reveal that all MDT samples contain free hydroxyl groups on their surface that play an important role for determining their catalytic activity [51]. These hydroxyl groups produce reactive OH radicals and provide active sites for the adsorption of pollutants [60]. Moreover, the identification of Ti-O, Ti-O-Ti and Ti-O-Mg bonds confirms the formation of magnesium doped titania among all the samples.

3.4 Scanning electron microscopy

The surface morphology of the MDT samples was studied using scanning electron microscopy at 2000x magnification and micrographs are shown in Figures 5 (a, b, c & d). The micrographs for MDT-1 and MDT-2 indicate that both the samples are composed of large aggregates of different sizes ranging from a few to several tens of microns resulted from tiny non-uniform shape crystals. These large aggregates further consist of small particles of numerous sizes and irregular shape randomly distributed on the surface which confirms the composite formation.

The surface morphology of MDT-3 significantly varies from MDT-1 and MDT-2 since it possesses a homogeneous structure with relatively less aggregation of particles. Moreover, spherical shape particles uniformly distributed on the surface of the sample can also be seen due to composite formation. Likewise, MDT-4 also bares spherical particles and fairly homogeneous structure of the composite with more agglomeration as compared to MDT-3.

Hence, the results reveal that as more quantity of magnesium dopant is induced in the titania matrix homogeneous structures with uniform shape of particles are obtained with the formation of small or large agglomerates. In fact, agglomerated surface morphologies with variable nanoparticle shapes and non-uniform sizes for sol-gel synthesized titania nanoparticles have been often reported by the previous scientists that indicates that these particles have tendency to agglomerate. The reason for this agglomeration is believed to be the high surface energy assimilated in the particles during their growth that tends to lower through aggregation [61].

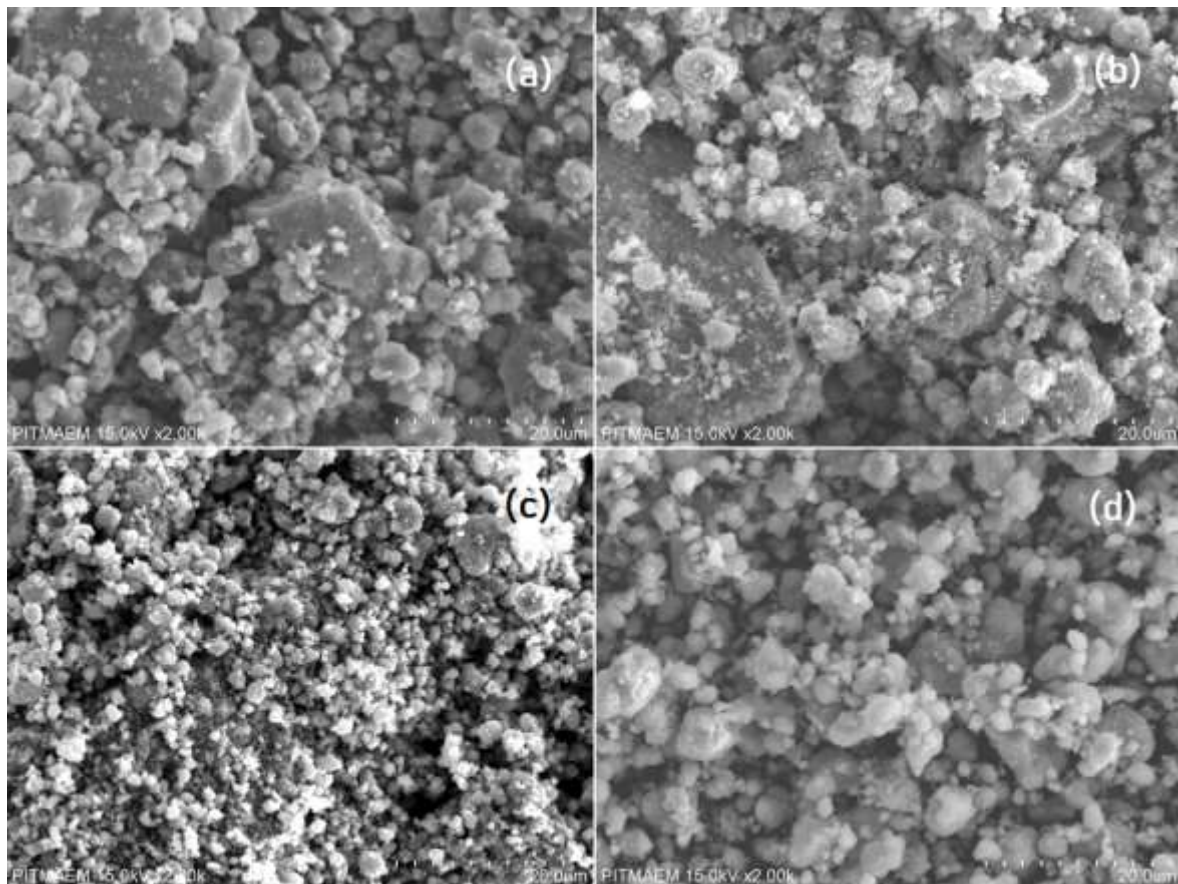


Figure 5: SEM micrographs (a) MDT-1; (b) MDT-2; (c) MDT-3; (d) MDT-4.

The researchers also found that the introduction of dopants in titania nanoparticles leads to strong aggregation especially doping with magnesium conditionally affects the crystallite size of titania and leads to the formation of microstructures with smaller grain size [62-64]. SHIVARAJU *et al.* observed that magnesium doped titania polyscales exhibit agglomerated spherical shaped particles with high surface area and porosity appropriate for improving photocatalytic activity against the degradation of dyes and other pollutants [35]. GALENDA and co-workers reported that all the prepared samples of boron and nitrogen doped titania

were obtained as agglomerates of micrometric sizes. According to them the samples composed of agglomerates larger than pure titania should be considered for better catalytic behavior [65]. AVASARALA *et al.* in the same way found fine crystals aggregated to form irregular shaped particles of magnesium doped titania catalyst with average size of 1.04 μm range [31]. CIFCI observed silver doped titania particles having different shapes of grains with irregular boundaries and many smaller crystals combined to form aggregates [66]. Similarly, Aware and co-workers obtained spherical shaped zinc doped titania nanoparticles with a slight agglomeration [67].

In some more researches, transition metals employed as dopants also lead to agglomeration of small nanocrystals with their irregular and non-homogeneous distribution as compared to pure titania. Moreover, this agglomeration seemed to increase significantly with increasing dopant metal [68-70].

3.5 Electron dispersive X-ray spectroscopy

The elemental composition of the prepared magnesium doped titanium dioxide samples was investigated by EDX spectroscopy. Figures 6a, 6b, 6c & 6d illustrate the EDX spectrum of MDT-1, MDT-2, MDT-3 and MDT-4 respectively.

The spectra along with Table 1 indicate the presence of titanium and oxygen as the major constituents among all the four MDT samples. However, magnesium can be seen in all the samples with the exception of MDT-1 that contains 1% magnesium as dopant since magnesium has not been detected in it probably due to the detection limit of EDX technique. The percentages of magnesium obtained for MDT-2, MDT-3 and MDT-4 are close to those calculated theoretically. Similarly, the molar ratios of titanium and oxygen are also in good agreement with the theoretical values. Hence, the results confirmed the successful doping of magnesium in titania matrix as well as the purity of synthesized MDT samples.

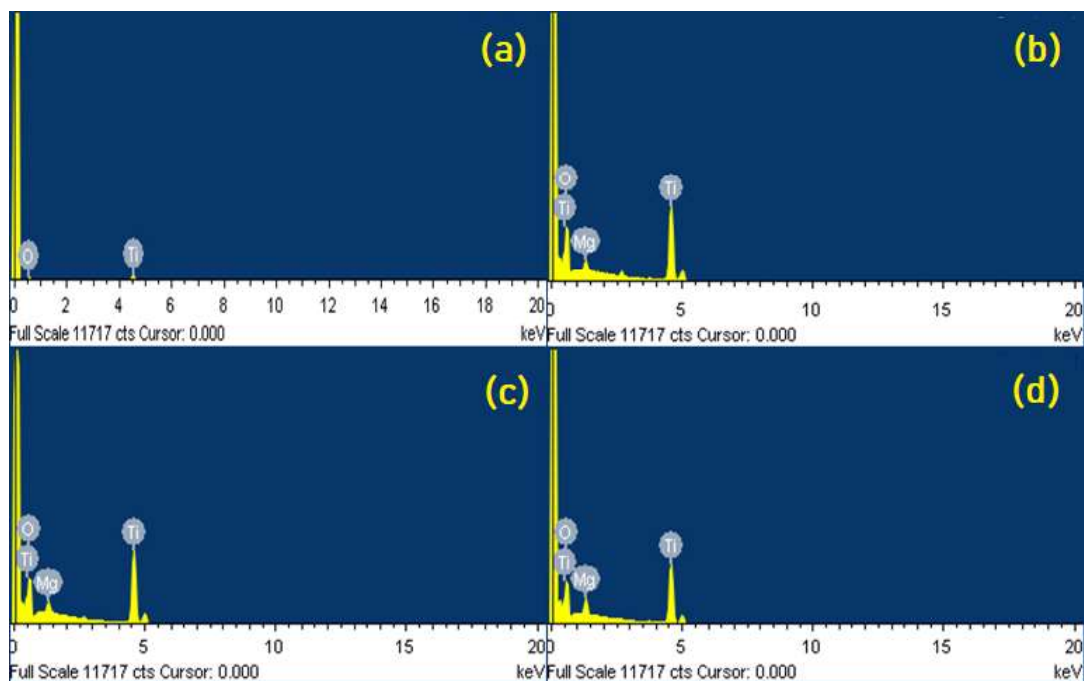


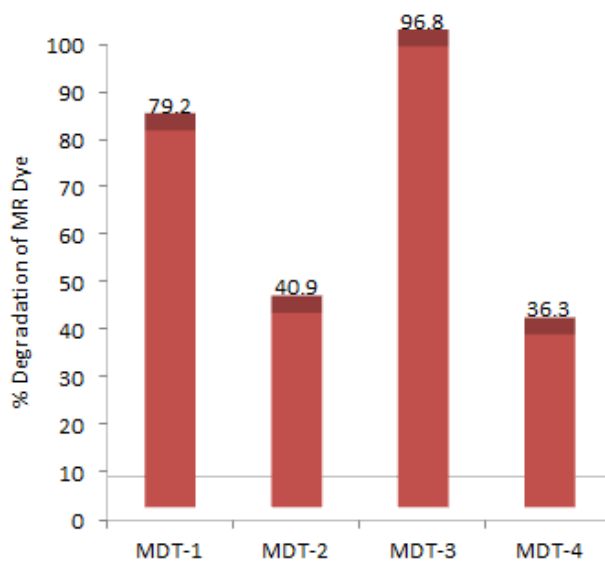
Figure 6: EDX analysis (a) MDT-1; (b) MDT-2; (c) MDT-3; (d) MDT-4.

Table 1: EDX Analysis-Elemental compositions of MDT samples.

Element	Weight %			
	MDT-1	MDT-2	MDT-3	MDT-4
O	46.46	49.52	46.93	46.44
Ti	53.54	48.11	50.33	48.88
Mg	--	2.37	2.74	4.68

3.6 Photocatalytic activity

In order to determine the photocatalytic efficiency of MDT samples and to find out an optimum dopant concentration for the degradation of MR solution, experiment was carried out by UV irradiating the suspension of 50 mg of each MDT catalyst added to 100 ml of 100 ppm methyl red aqueous solution for one hour. The residual methyl red concentrations were quantified by the absorption studies and the results are shown in Figures 6. The figure shows that MDT-1 degraded a substantial quantity of MR dye i.e. 79.2% but MDT-2 on the other hand, exhibited less significant behavior towards degradation of methyl red dye i.e. 40.9%. However, MDT-3 showed maximum photocatalytic activity with 96.8% dye degradation. MDT-4 again had 36.3% dye degradation after 60 minutes of UV irradiation. MDT-3 showed maximum result for dye degradation because of its homogeneous structure and uniform morphology of particles with less aggregation while all other MDT samples are composed of larger aggregates.


Figure 7: Photocatalytic degradation of methyl red dye.

It can be seen from these results that minimum percentage of dye degradation was observed in case of MDT-4 having 5% of magnesium metal in titania matrix. The reason being that the metal content diffuses into titania matrix up to a certain limit therefore at higher concentrations it starts depositing on the surface of titania thereby hindering the UV light penetration and subsequently reducing the photocatalytic activity [70]. Similar is the case with the dye that sometimes it only adsorbs on the surface of catalyst instead of being degraded depending upon the surface-dye electrostatic interactions and consequently reduces the interaction between MR and titania due to hindrance created for the incident UV radiation and leads to slower dye degradation. Many authors believe the adsorption to be an essential step. Initial equilibration time before starting the UV irradiation being an important factor, in the present study preliminary stirring in the dark for 30 minutes plays an important role in the adsorption of dye [65].

Previous scientists reported that doping of metal ions into titania matrix serves as a moderator of the interfacial charge transfer as well as a recombination centre therefore high dye degradation rates are obtained at optimal dopant concentration levels. AVASARALA *et al.* observed that doping of even minor quantities of

magnesium ions in titania matrix strongly influence the photocatalytic activity and increases it but up to a certain limit i.e. 1%; further increase in magnesium ions doping becomes disadvantageous [31]. Similarly, SHIVARAJU and co-workers compared Mg-doped titania polyscales with pure titania and found it to be more efficient photocatalyst for the degradation of industrial dyes like methyl violet, methyl red, methyl orange, brilliant green and brilliant blue with 100%, 80%, 79%, 73% and 64% dye degradation respectively [35]. In a study Cifci observed that maximum degradation for methylene blue and methyl orange was achieved with titania nanoparticles doped with 1% silver ions that decreased with further increase in dopant concentration [66].

In fact these observations regarding the photocatalytic activity of a catalyst are attributed to a few influential factors including the oxygen vacancies created by the dopant ions on the surface of titania which entangle the photoinduced electrons but at higher concentrations of doped metal ions the oxygen vacancies exceed to such a limit that they become recombination cores of photogenerated electrons and holes insignificant for the activity of a photocatalyst. Another factor is the electronegativity difference between the host metal and the doped metal, more the electronegativity difference between the two metals more the charge transfer and hence increased photocatalytic activity. One more significant factor is the deformation caused by the doped metal in the framework of host matrix that causes defects resulting in inhibition of the recombination of electron-hole pairs and subsequent enhanced photocatalytic activity [70]. DIVYA *et al.* reported concentration dependence of dye degradation since in a series of experiments they observed that using copper doped titania, Orange II dye ranging from 50 to 400 ppm aqueous solutions degrades fast at lower concentrations and takes longer time at higher concentrations probably due to color hindrance in penetration of light into the reaction sample [71].

4. CONCLUSIONS

In conclusion, it can be said that pure magnesium doped titania composites were synthesized by the aqueous route of simple and the most feasible sol-gel process. The synthesis was carried out at a low temperature i.e. 60 °C and the calcination step to induce crystallinity was also done at a moderate temperature i.e. 500 °C. The X-ray diffraction analysis revealed that both anatase and rutile phases of titania exist among MDT-1, MDT-2 and MDT-3 but the rutile phase diminished as the percentage of dopant was increased till it disappeared completely in MDT-4 comprising of the single anatase phase. So, the first three samples contained mixed phases suitable for enhancing the photocatalytic activity of titania. Moreover, the cubic phase of magnesium oxide detected among all the samples proved its doping into the titania matrix.

DSC-TGA performed from room temperature to 1000 °C indicated a maximum weight loss of 30.91% in case of MDT-1 that reduced to 10.58%, 6.67% and 4.67% for MDT-2, MDT-3 and MDT-4 respectively proving the thermal stability of composites with the increase in percentage of dopant. Infrared spectroscopy identified the presence of free surface hydroxyl groups, Ti–O, Ti–O–Ti and Ti–O–Mg bonds in case of all the samples. Scanning electron microscopy showed that as the quantity of magnesium dopant in titania matrix was increased the agglomeration decreased and as a result homogeneous structures were formed. Therefore, the ability of sol-gel prepared titania nanostructures to agglomerate can be regulated by introducing minor quantities of metal dopant into titania matrix. EDX analysis also confirmed the purity and doping of magnesium in the titania matrix. The photocatalytic activity evaluation of synthesized MDT catalysts against methyl red dye confirmed their efficacy for use as photocatalysts though agglomeration of crystals, deposition of dopant and oxygen vacancies on the titania surface strongly influence the photocatalytic activity. It was observed that out of all the four samples, MDT-3 having 3% magnesium showed maximum degradation i.e. 96.8%. Hence, the study reveals successful synthesis of magnesium doped titania photocatalyst.

5. BIBLIOGRAPHY

- [1] SIWINSKA-STEFANSKA, K., PAUKSZTA, D., PIASECKI, A., *et al.*, “Synthesis and physicochemical characteristics of titanium dioxide doped with selected metals,” doi: 10.5277/ppmp140122. *Physicochemical Problems of Mineral Processing*, v. 50, n. 1, pp. 265-276, 2014.
- [2] GUAN, D., *et al.*, “Aerosol synthesis of trivalent titanium doped titania/carbon composite microspheres with superior sodium storage performance,” doi: 10.1007/s12274-017-1675-3. *Nano Research*, v. 10, n. 12, pp. 4351-4359, Dec. 2017.

- [3] TARQUINIO, K., “Bactericidal effects of silver plus titanium dioxide-coated endotracheal tubes on *Pseudomonas aeruginosa* and *Staphylococcus aureus*,” *International Journal of Nanomedicine*, p. 177, Mar. 2010, doi: 10.2147/IJN.S8746.
- [4] ATHIRA, K., MERIN, K.T., RAGURAM, T., *et al.*, “Synthesis and characterization of Mg doped TiO₂ nanoparticles for photocatalytic applications,” doi: 10.1016/j.matpr.2020.04.580. *Materials Today: Proceedings*, v. 33, pp. 2321-2327, 2020.
- [5] SUN, T., HAO, H., HAO, W., *et al.*, S. “Preparation and antibacterial properties of titanium-doped ZnO from different zinc salts,” doi: 10.1186/1556-276X-9-98. *Nanoscale Research Letters*, v.9, n. 1, p. 98, Dec. 2014.
- [6] CHUNG, W. O., WATAHA, J., C., HOBBS, D.T., “Mini Review: Novel antimicrobial compounds in the age of increasing bacterial resistance,” *Science against microbial pathogens: communicating current research and technological advances A. Méndez-Vilas (Ed.)*, pp. 722-727, Formatex, Spain, 2011.
- [7] MOHSENI, S., AGHAYAN, M., GHORANI-AZAM, A., *et al.*, “Evaluation of antibacterial properties of Barium Zirconate Titanate (BZT) nanoparticle,” doi: 10.1590/S1517-83822014000400033. *Brazilian Journal of Microbiology*, v. 45, n. 4, pp. 1393-1399, Dec. 2014.
- [8] STEPANOV, A.L., “Applications of ion implantation for modification of TiO₂: A REVIEW,” *Rev. Adv. Mater. Sci.*, v. 30, pp. 150-165, 2012.
- [9] DUYZMAZ, B., YIGIT, Z.V., ŞEKER, M.G., *et al.*, “Antibacterial Properties of Sol-Gel Derived TiO₂ Nanoparticles,” doi: 10.12693/APhysPolA.129.872. *Acta Physica Polonica A*, v. 129, n. 4, pp. 872-874, Apr. 2016.
- [10] KEDZIORA, A., STREK, W., KEPINSKI, L., *et al.*, “Synthesis and antibacterial activity of novel titanium dioxide doped with silver,” doi: 10.1007/s10971-012-2688-8. *Journal of Sol-Gel Science and Technology*, v. 62, n. 1, pp. 79-86, Apr. 2012.
- [11] GUPTA, K., SINGH, R.P., PANDEY, A., *et al.*, “Photocatalytic antibacterial performance of TiO₂ and Ag-doped TiO₂ against *S. aureus*, *P. aeruginosa* and *E. coli*,” doi: 10.3762/bjnano.4.40. *Beilstein Journal of Nanotechnology*, v. 4, pp. 345-351, Jun. 2013.
- [12] TOBALDI, D.M., *et al.*, “Silver-Modified Nano-titania as an Antibacterial Agent and Photocatalyst,” doi: 10.1021/jp411997k. *The Journal of Physical Chemistry C*, v. 118, n. 9, pp. 4751-4766, Mar. 2014.
- [13] GOERNE, T.M.L., LEMUS, M.M., MORALES, V.A., *et al.*, “Study of Bacterial Sensitivity to Ag-TiO₂ Nanoparticles,” doi: 10.4172/2157-7439.S5-003. *Journal of Nanomedicine & Nanotechnology*, v. 5, n. 01, 2011.
- [14] STOYANOVA, A.M., HITKOVA, H.Y., IVANOVA, N.K., *et al.*, “Photocatalytic and antibacterial activity of Fe-doped TiO₂ nanoparticles prepared by nonhydrolytic sol-gel method,” *Bulgarian Chemical Communications*, v. 45, n. 4, pp. 497-504, 2013.
- [15] STOYANOVA, D., IVANOVA, I., ANGELOV, O., *et al.*, “Antibacterial activity of thin films TiO₂ doped with Ag and Cu on Gracilicutes and Firmicutes bacteria,” doi: 10.3897/biodiscovery.20.e21596. *BioDiscovery*, v. 20, p. e21596, Dec. 2017.
- [16] CHEKURI, R.D., TIRUKKOVALLURI, S. R., “Synthesis Of Cobalt Doped Titania Nano Materials Assisted By Anionic Heterogemini Surfactants: Characterization And Its Applications In Heterogeneous Photocatalysis And Antibacterial Activity,” 2016. [Online]. Available: www.ijera.com.
- [17] MANZOOR, M., RAFIQ, A., IKRAM, M., *et al.*, “Structural, optical, and magnetic study of Ni-doped TiO₂ nanoparticles synthesized by sol-gel method,” doi: 10.1007/s40089-018-0225-7. *International Nano Letters*, v. 8, n. 1, pp. 1-8, Mar. 2018.
- [18] ZANE, A., *et al.*, “Biocompatibility and antibacterial activity of nitrogen-doped titanium dioxide nanoparticles for use in dental resin formulations,” doi: 10.2147/IJN.S117584. *International Journal of Nanomedicine*, v. 11, pp. 6459-6470, Dec. 2016.
- [19] MUNGONDORI, H., TICHAGWA, L., GREEN, E., “Synthesis and Glass Immobilization of Carbon and Nitrogen Doped TiO₂-SiO₂ and Its Effect on *E. coli* ATCC 25922 Bacteria,” doi: 10.9734/bjast/2015/11049. *British Journal of Applied Science & Technology*, v. 5, n. 5, pp. 447-460, Jan. 2015.
- [20] WONG, M.-S., *et al.*, “Visible-Light-Induced Bactericidal Activity of a Nitrogen-Doped Titanium Photocatalyst against Human Pathogens,” doi: 10.1128/AEM.02580-05. *Applied and Environmental Microbiology*, v. 72, n. 9, pp. 6111-6116, Sep. 2006.
- [21] LI, R., JIN, T., LIU, Z., *et al.*, “Antimicrobial Double-Layer Coating Prepared from Pure or Doped-Titanium Dioxide and Binders,” doi: 10.3390/coatings8010041. *Coatings*, v. 8, n. 1, p. 41, Jan. 2018.
- [22] MHA, R., and J, A., “TiO₂/Polymer Nanocomposites for Antibacterial Packaging Application,” doi: 10.15744/2639-3328.1.101. *Journal of Advancements in Food Technology*, v. 1, n. 1, Aug. 2018.
- [23] RIAZIAN, M., “Electrical properties and enhancement of photocatalytic activity of TiO₂ nanorods doped with SiO₂,” doi: 10.17159/0379-4350/2017/v70a26. *South African Journal of Chemistry*, v. 70, pp. 189-199, 2017.

- [24] CENDROWSKI, K., “Mesoporous Silica Nanospheres Functionalized by TiO₂ as a Photoactive Antibacterial Agent,” doi: 10.4172/2157-7439.1000182. *Journal of Nanomedicine & Nanotechnology*, v. 04, n. 6, 2013.
- [25] LI, J., XIE, B., XIA, K., *et al.*, “Enhanced Antibacterial Activity of Silver Doped Titanium Dioxide-Chitosan Composites under Visible Light,” doi: 10.3390/ma11081403. *Materials*, v. 11, n. 8, pp. 1403, Aug. 2018.
- [26] ALBERT, E., *et al.*, “Antibacterial properties of Ag-TiO₂ composite sol-gel coatings,” doi: 10.1039/C5RA05990A. *RSC Advances*, vol. 5, n. 73, pp. 59070-59081, 2015.
- [27] YU, B., LEUNG, K.M., GUO, Q., *et al.* “Synthesis of Ag-TiO₂ composite nano thin film for antimicrobial application,” doi: 10.1088/0957-4484/22/11/115603. *Nanotechnology*, v. 22, n. 11, p. 115603, Mar. 2011.
- [28] MOONGRAKSATHUM, B., SHANG, J.-Y., CHEN, Y.-W., “Photocatalytic Antibacterial Effectiveness of Cu-Doped TiO₂ Thin Film Prepared via the Peroxo Sol-Gel Method,” doi: 10.3390/catal8090352. *Catalysts*, v. 8, n. 9, p. 352, Aug. 2018.
- [29] DUNNILL, C.W., *et al.*, “White light induced photocatalytic activity of sulfur-doped TiO₂ thin films and their potential for antibacterial application,” doi: 10.1039/b913793a. *Journal of Materials Chemistry*, v. 19, n. 46, pp. 8747, 2009.
- [30] WONG, M.-S., SUN, D.-S., CHANG, H.-H., “Bactericidal Performance of Visible-Light Responsive Titania Photocatalyst with Silver Nanostructures,” doi: 10.1371/journal.pone.0010394. *PLoS ONE*, v. 5, n. 4, pp. e10394, Apr. 2010.
- [31] AVASARALA, B.K., TIRUKKOVALLURI, S.R., “Magnesium Doped Titania for Photocatalytic Degradation of Dyes in Visible Light,” doi: 10.4172/2161-0525.1000358. *Journal of Environmental & Analytical Toxicology*, v. 06, n. 2, 2016.
- [32] ISMAIL, M.A., HEDHILI, M. N., ANJUM, D.H., *et al.*, “Synthesis and Characterization of Iron-Doped TiO₂ Nanoparticles Using Ferrocene from Flame Spray Pyrolysis,” doi: 10.3390/catal11040438. *Catalysts*, v. 11, n. 4, pp. 438, Mar. 2021,
- [33] WONG, M.-S., CHEN, C.-W., HSIEH, C.-C., *et al.*, “Antibacterial property of Ag nanoparticle-impregnated N-doped titania films under visible light,” doi: 10.1038/srep11978. *Scientific Reports*, v. 5, no. 1, p. 11978, Dec. 2015.
- [34] BAGHERI, S., SHAMELI, K., ABD HAMID, S.B., “Synthesis and Characterization of Anatase Titanium Dioxide Nanoparticles Using Egg White Solution via Sol-Gel Method,” doi: 10.1155/2013/848205. *Journal of Chemistry*, v. 2013, 2013.
- [35] SHIVARAJU, H.P., MIDHUN, G., KUMAR, K.M.A., PALLAVI,S., *et al.*, “Degradation of selected industrial dyes using Mg-doped TiO₂ polyscales under natural sun light as an alternative driving energy,” doi: 10.1007/s13201-017-0546-0. *Applied Water Science*, v. 7, n. 7, pp. 3937–3948, Nov. 2017.
- [36] ABDULMAJEED, I.M., CHYAD, F.A., ABBAS, M.M., *et al.*, “Fabrication and Characterization of Ultrafine Crystalline MgO and ZnO Powders,” 2007. [Online]. Available: www.ijirset.com.
- [37] SHARMA, G., SONI, R., JASUJA, N.D., “Phytoassisted synthesis of magnesium oxide nanoparticles with *Swertia chirayaita*,” doi: 10.1016/j.jtusc.2016.09.004. *Journal of Taibah University for Science*, v. 11, n. 3, pp. 471-477, May 2017.
- [38] KEITEB, A., SAION, E., ZAKARIA, A., *et al.*, “A Modified Thermal Treatment Method for the Up-Scalable Synthesis of Size-Controlled Nanocrystalline Titania,” doi: 10.3390/app6100295. *Applied Sciences*, v. 6, n. 10, pp. 295, Oct. 2016.
- [39] ZOCCAL, J.V.M., AROUCA, F.O., GONÇALVES, J.A.S., “Synthesis and Characterization of TiO₂; Nanoparticles by the Method Pechini,” doi: 10.4028/www.scientific.net/MSF.660-661.385. *Materials Science Forum*, v. 660-661, pp. 385-390, Oct. 2010.
- [40] NYAMUKAMBA, P., OKOH, O., TICHAGWA, L,*et al.*, “Preparation of Titanium Dioxide Nanoparticles Immobilized on Polyacrylonitrile Nanofibres for the Photodegradation of Methyl Orange,” doi: 10.1155/2016/3162976. *International Journal of Photoenergy*, v. 2016, 2016.
- [41] BA-ABBAD, M.M., KADHUM, A.H.A., MOHAMAD, A.B.,*et al.*, “Synthesis and Catalytic Activity of TiO₂ Nanoparticles for Photochemical Oxidation of Concentrated Chlorophenols under Direct Solar Radiation,” 2012. [Online]. Available: www.electrochemsci.org.
- [42] ALAMGIR, KHAN, W., AHMAD, S., *et al.*, “Thermal analysis and temperature dependent dielectric responses of Co doped anatase TiO₂ nanoparticles”, doi: 10.1063/1.4915355. *Proceedings of the International Conference on Condensed Matter Physics 2014 (ICCMP 2014)*,” 2015, pp. 010001.
- [43] SWAPNA, M.V., HARIDAS, K.R., “An easier method of preparation of mesoporous anatase TiO₂ nanoparticles via ultrasonic irradiation,” doi: 10.1080/17458080.2015.1094189. *Journal of Experimental Nanoscience*, v. 11, n. 7, pp. 540-549, May 2016.

- [44] MEHRANPOUR, H., ASKARI, M., GHAMSARI, M.S., *et al.*, “Study on the Phase Transformation Kinetics of Sol-Gel Driven TiO₂ Nanoparticles,” doi: 10.1155/2010/626978. *Journal of Nanomaterials*, v. 2010, 2010.
- [45] MARINESCU, C., *et al.*, “DSC investigation of nanocrystalline TiO₂ powder,” doi: 10.1007/s10973-010-1072-6. *Journal of Thermal Analysis and Calorimetry*, v. 103, n. 1, pp. 49-57, Jan. 2011.
- [46] PULIŠOVÁ, P., *et al.*, “Thermal behaviour of titanium dioxide nanoparticles prepared by precipitation from aqueous solutions,” doi: 10.1007/s10973-010-0893-7. *Journal of Thermal Analysis and Calorimetry*, v. 101, n. 2, pp. 607-613, Aug. 2010.
- [47] KIM, C.S., NAKASO, K., XIA, B., *et al.*, “A New Observation on the Phase Transformation of TiO₂ Nanoparticles Produced by a CVD Method,” doi: 10.1080/027868290906986. *Aerosol Science and Technology*, v. 39, n. 2, pp. 104-112, Feb. 2005.
- [48] YODYINGYONG, S., SAE-KUNG, C., PANIJPAN, B., *et al.*, “Physicochemical properties of nanoparticles titania from alcohol burner calcination” doi: 10.4314/bcse.v25i2.65901. *Bulletin of the Chemical Society of Ethiopia*, v. 25, n. 2, May 2011.
- [49] MEI, L.F., LIANG, K.M., “Crystallization Behavior of Mg-Doped Titania,” doi: 10.4028/www.scientific.net/KEM.434-435.847. *Key Engineering Materials*, v. 434-435, pp. 847-849, Mar. 2010.
- [50] HEMA, M., ARASI, A. Y., TAMILSELVI, P., *et al.*, “Titania Nanoparticles Synthesized by Sol-Gel Technique,” doi: 10.7598/cst2013.344. *Chemical Science Transactions*, v. 2, n. 1, Nov. 2012.
- [51] ŠČEPANOVIĆ, M., *et al.*, “Photocatalytic degradation of metoprolol in water suspension of TiO₂ nanopowders prepared using sol-gel route,” doi: 10.1007/s10971-011-2639-9. *Journal of Sol-Gel Science and Technology*, v. 61, n. 2, Feb. 2012.
- [52] LOPEZ-ISCOA, P., *et al.*, “Design, Synthesis, and Structure-Property Relationships of Er³⁺-Doped TiO₂ Luminescent Particles Synthesized by Sol-Gel,” doi: 10.3390/nano8010020. *Nanomaterials*, v. 8, n. 1, p. 20, Jan. 2018.
- [53] RAMIMOGHADAM, D., BAGHERI, S., ABD HAMID, S.B., “Biotemplated Synthesis of Anatase Titanium Dioxide Nanoparticles via Lignocellulosic Waste Material,” doi: 10.1155/2014/205636. *BioMed Research International*, v. 2014, 2014.
- [54] CHEKURI, R.D., TIRUKKOVALLURI, S.R., “Synthesis of cobalt doped titania nano material assisted by gemini surfactant: Characterization and application in degradation of Acid Red under visible light irradiation,” doi: 10.1016/j.sajce.2017.10.001. *South African Journal of Chemical Engineering*, v. 24, pp. 183-195, Dec. 2017.
- [55] MESHESHA, D.S., MATANGI, R.C., TIRUKKOVALLURI, S.R., *et al.*, “Synthesis and characterization of Ba²⁺ and Zr⁴⁺ co-doped titania nanomaterial which in turn used as an efficient photocatalyst for the degradation of rhodamine-B in visible light,” doi: 10.1016/j.sajce.2016.10.004. *South African Journal of Chemical Engineering*, v. 23, pp. 10-16, Jun. 2017.
- [56] AHMAD, S., SAEED, A., “Synthesis of Metal/Silica/Titania Composites for the Photocatalytic Removal of Methylene Blue Dye,” doi: 10.1155/2019/9010289. *Journal of Chemistry*, v. 2019, pp. 1-6, Feb. 2019.
- [57] TRIVEDI, M.K., TRIVEDI, A.B.D., “Spectroscopic Characterization of Disodium Hydrogen Orthophosphate and Sodium Nitrate after Biofield Treatment,” doi: 10.4172/2157-7064.1000282. *Journal of Chromatography & Separation Techniques*, v. 06, n. 05, 2015.
- [58] KEERTHANA, B., MADHAVAN, J., THALAPATHI, M.A., “Optical Properties of Pure and Gd³⁺-Doped Titanium Dioxide,” 2015, [Online]. Available: www.ijedr.org.
- [59] LIU, S.Y., YANG, H.Y., MIN, *et al.*, “Solid-State Synthesis and Thiophanate Methyl Visible Light Degradation of Magnesium Doped TiO₂ Mesoporous Nanomaterial,” doi: 10.4028/www.scientific.net/MSF.789.18. *Materials Science Forum*, v. 789, pp. 18-27, Apr. 2014.
- [60] OCWELWANG, A., TICHAGWA, L., OCWELWANG, A.R., “Synthesis and characterisation of Ag and nitrogen doped TiO₂ nanoparticles supported on a Chitosan-PVAE nanofibre support Water Treatment View project Development of Super hydrophobic self-cleaning surfaces View project Synthesis and Characterisation of Ag and Nitrogen Doped TiO₂ Nanoparticles Supported on A Chitosan-Pvae Nanofibre Support,” *International Journal of Advanced Research in Chemical Science (IJARCS)*, v. 1, n. 2, pp. 28–37, 2014, [Online]. Available: <https://www.researchgate.net/publication/269631961>.
- [61] SRIVASTAVA, N., SRIVASTAVA, P.C., “Realizing NiO nanocrystals from a simple chemical method,” doi: 10.1007/s12034-011-0142-0. *Bulletin of Materials Science*, v. 33, n. 6, pp. 653-656, Dec. 2010.
- [62] ZIEMKOWSKA, W., BASIAK, D., KURTYCZ, P., *et al.*, “Nano-titanium oxide doped with gold, silver, and palladium - synthesis and structural characterization,” doi: 10.2478/s11696-014-0537-7. *Chemical Papers*, v. 68, n. 7, Jan. 2014.

- [63] KHAIRY, M., ZAKARIA, W., “Effect of metal-doping of TiO₂ nanoparticles on their photocatalytic activities toward removal of organic dyes,” doi: 10.1016/j.ejpe.2014.09.010. *Egyptian Journal of Petroleum*, v. 23, n. 4, pp. 419-426, Dec. 2014.
- [64] KAVIYARASU, K., PREMANAND, D., KENNEDY, J., *et al.*, “Synthesis of doped TiO₂ nanocrystals prepared by wet-chemical method: optical and microscopic studies,” doi: 10.1142/S0219581X13500336. *International Journal of Nanoscience*, v. 12, n. 05, p. 1350033, Oct. 2013.
- [65] GALENDA, A., CROCIANI, L., HABRA, N.El., *et al.*, “Effect of reaction conditions on methyl red degradation mediated by boron and nitrogen doped TiO₂,” doi: 10.1016/j.apsusc.2014.06.175. *Applied Surface Science*, v. 314, pp. 919-930, Sep. 2014.
- [66] ÇIFÇI, D.İ., “Decolorization of methylene blue and methyl orange with Ag doped TiO₂ under UV-A and UV-Visible conditions: process optimization by response surface method and toxicity evaluation,” doi: 10.30955/gnj.001899. *Global NEST Journal*, v. 18, n. 2, pp. 371-380, May 2016.
- [67] AWARE, D.V., JADHAV, S.S., “Synthesis, characterization and photocatalytic applications of Zn-doped TiO₂ nanoparticles by sol-gel method,” doi: 10.1007/s13204-015-0513-8. *Applied Nanoscience*, v. 6, n. 7, pp. 965-972, Oct. 2016.
- [68] GONELL, F., PUGA, A.V., JULIÁN-LÓPEZ B., *et al.*, “Copper-doped titania photocatalysts for simultaneous reduction of CO₂ and production of H₂ from aqueous sulfide,” doi: 10.1016/j.apcatb.2015.06.019. *Applied Catalysis B: Environmental*, v. 180, pp. 263-270, Jan. 2016.
- [69] OGANISIAN, K., HRENIK, A., SIKORA, A., *et al.*, “Synthesis of iron doped titanium dioxide by sol-gel method for magnetic applications,” doi: 10.2298/PAC1501043O. *Processing and Application of Ceramics*, v. 9, n. 1, pp. 43-51, 2015.
- [70] THU, T.N.T., THI, N.N.V. QUANG, T.K., *et al.*, “Synthesis, characterisation, and effect of pH on degradation of dyes of copper-doped TiO₂,” doi: 10.1080/17458080.2015.1053541. *Journal of Experimental Nanoscience*, v. 11, n. 3, pp. 226-238, Feb. 2016.
- [71] DIVYA, N., BANSAL, A., JANA, A.K., “Photocatalytic degradation of azo dye Orange II in aqueous solutions using copper-impregnated titania,” doi: 10.1007/s13762-013-0238-8. *International Journal of Environmental Science and Technology*, v. 10, n. 6, pp. 1265-1274, Nov. 2013.

ORCID

Samreen Zahra	https://orcid.org/0000-0001-5504-7816
Sania Mazhar	https://orcid.org/0000-0003-0691-8528
Sarwat Zahra	https://orcid.org/0000-0001-8901-6639
Hira Idrees	https://orcid.org/0000-0002-6048-142X
Ali Hussnain	https://orcid.org/0000-0001-5377-6302